



# Virtual Acoustics of the Cathedral of Malaga (Spain)

L. Álvarez, A. Alonso, T. Zamarreño, S. Girón, and M. Galindo.

Instituto Universitario de Arquitectura y Ciencias de la Construcción, Universidad de Sevilla, Av. Reina Mercedes, 2, E. T. S. de Arquitectura, 41012 Sevilla, Spain.

## Summary

The Catholic Cathedral of Malaga (southern Spain), located in the historical centre, is the most emblematic building of the city. Its construction began in 1528 and was completed in 1782, suffering several interruptions and modifications at the hands of various architects, and hence various architectural styles are superimposed: the interior is Renaissance and the façade is predominantly Baroque. Rectangular in shape, it has three naves of the same height, with the central nave being the widest. In this work, a 3D model of this ecclesiastical space is created in order to carry out an acoustic simulation of its sound field by using the simulation algorithms of CATT Acoustic software implemented in the new TUCT calculation motor (The Universal Cone Tracer). The virtual model created is calibrated through an iterative process of adjustment of reverberation times simulated in such a way that they differ by no more than 5% from those measured. These measured values were obtained from the impulse responses monitored in situ. Likewise, a comparison of the experimental and simulated results of other acoustic parameters in terms of their just noticeable differences (JND) was also carried out, which supports the reliability of the computational acoustic model implemented. This work is the starting point of a multidisciplinary project which aims to incorporate the acoustic aspects within the heritage value of Andalusian cathedrals.

PACS no. 43.55.Gx, 43.55.ka

## 1. Introduction

Computational models [1] based on geometric acoustics first appeared in around 1967, and since the early 90s they have succeeded in attaining results ever closer to the true acoustic conditions of a closed enclosure. Thanks to improvements in both the calculation speed of hardware and in equipment technology, and to the appearance of new software, these techniques currently provide highly reliable results despite the limitations commonly associated with geometric models. The latest improvements include algorithms capable of producing auralizations of high quality [2].

The general computational base is the raytracing technique, whose accuracy requires the detailed description of the full acoustic properties of the surfaces. Various algorithms have been developed to implement the propagation of the acoustic energy inside an enclosure by using raytracing

techniques. In particular, the algorithm of raytracing [3] is based on the trace and pursuit of the sound rays from a point of the enclosure that acts as the source, up to the reception point, by following the laws of geometric optics, and takes up to a certain order of reflections into account. The method has since been further developed and the path of each ray has become a circular cone [4], or pyramidal with a triangular base [5]. The algorithm of the image sources is used to generate an echogram by bearing in mind the intensity associated to each reflection and the time of arrival in relation to the direct sound. When arbitrary surfaces exist then the number of possible images increases exponentially with the reflection order, resulting in a complicated model, as occurs in concert halls. In 1989, Vorländer [6] presented the first hybrid algorithm in an attempt to combine the advantages of previous algorithms and to limit the incidence of their drawbacks. This technique has been applied successfully by some authors in different types of buildings, particularly in Catholic churches [7, 8].



Figure 1. Aerial view of the Cathedral of Malaga.



Figure 2. Interior view of the main altar.

This work focuses on the presentation of the calibrated and validated computational model created from the interior space of Malaga Cathedral, as the first results of an interdisciplinary research project which aims to conduct a detailed acoustic study of the main cathedrals of the region (Andalusia). This scientific knowledge will constitute a new contribution to the rich heritage of these buildings, by incorporating the acoustic assessment compared to the traditional stylistic-functional vision, recognized as Intangible Heritage.

## 2. Description of the Cathedral

Located in the historical centre, the Catholic Cathedral of Malaga (southern Spain) [9], is the most emblematic building of the city. Its construction lasted from 1528 when work was initiated on the principal mosque in the Islamic city at the time, until 1782, ending a long building process caught up in constant interruptions and modifications under the direction of different architects, and hence various architectural styles are superimposed on the building: the interior is Renaissance and the façade is predominantly Baroque. Although it was designed with two towers, only one tower was actually built (see Figure 1).

The interior of the cathedral is of Renaissance style: a basilica ground plan (rectangular) with three naves of the same height, with the central nave the widest. The entire temple is supported by large pillars covered by columns with a capital from which new pillars with pilasters emerge that support a network of semicircular domes. The height of these domes is approximately 42 m from the floor. Light penetrates the interior by the triple arches open at the height of the second body

through the windows and also through the chapel windows.

The presbytery located in the apse of the temple is raised and surrounded by walls cut by high windows between fluted Corinthian columns and topped with a beautiful ribbed vault. The pulpits, made of marble, are placed near the high altar. In the lateral spaces of the naves and around the apse there are chapels, each of which boasts its own altar.

The choir is situated in the centre of the temple flanked by two large organs, furnished with wooden seating carved by Pedro de Mena, and with various altars with wooden and marble sculptures. The ground plan of the cathedral (Figure 3) shows the location of the most important places mentioned, plus the chapels, and the positions for the reception of the microphones (19 in total) and for the sound source (S) for the acoustic measurements and simulations.

The cathedral has white and red jasper marble flooring. The columns supporting the lower and upper galleries are of limestone, and the domes and the chapel walls are made of stone. The inner doors in the transept are made of pine. The presbytery is carpeted and there are wooden pews and plastic chairs in the congregational seating zones (Figure 3).

## 3. Experimental technique

The procedures employed here are those established in the ISO 3382-1 standard [10] and measurements were carried out in the unoccupied temple. Temperature and relative humidity were monitored while measurements were taken by a precision electronic thermo-hygrometer.

The impulse responses (IR) were obtained at each reception point using sine sweep signals which were generated and analysed by the EASERA [11]

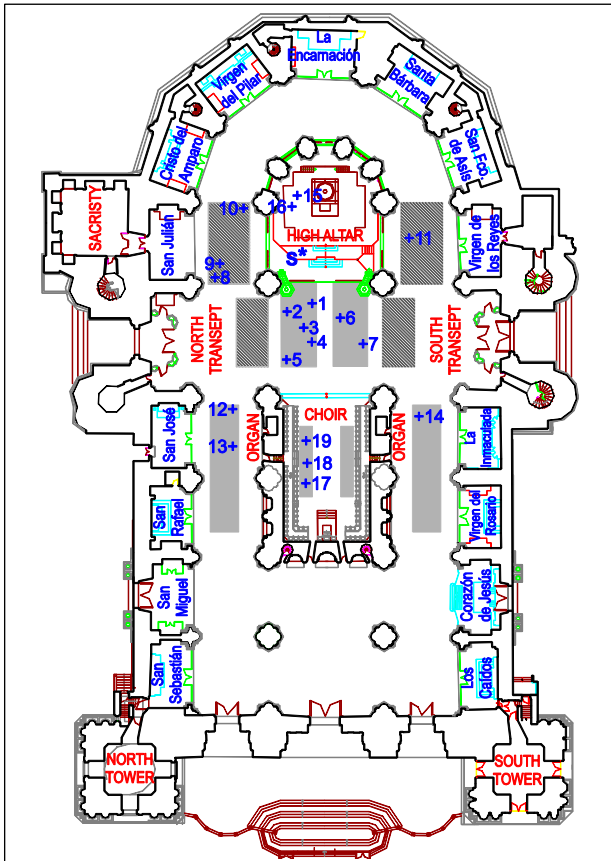


Figure 3. Ground plan of the Cathedral showing the pew (grey) and chair (dashed grey) zones for the congregation and the positions of the source (S) and microphone.

software via the sound card Roland Edirol UA-25EX. The omnidirectional source, a Rivas RSAN-AG dodecahedral loudspeaker with a Behringer Europower EP2500 amplifier, is placed at the most usual point of location of the natural source (S) in the high altar at a height of 1.70 m from the floor. The omnidirectional microphone Audix TR40 captured the sound signals and was located at the approximate height of the ears of a seated person, 1.20 m from the floor, at a predetermined number of positions (numbered from 1 to 19) in the congregational zones (see Figure 3).

These monaural IRs were measured to determine the following acoustic parameters for each frequency octave band between 125 Hz to 4000 Hz and in all receiver positions: reverberation times ( $T_{20}$ ), early decay time (EDT), centre time ( $T_S$ ), clarity ( $C_{80}$ ), and definition ( $D_{50}$ ).

#### 4. Acoustic simulation

The software used for the acoustic simulation is CATT-Acoustic [12]. The full detailed calculation

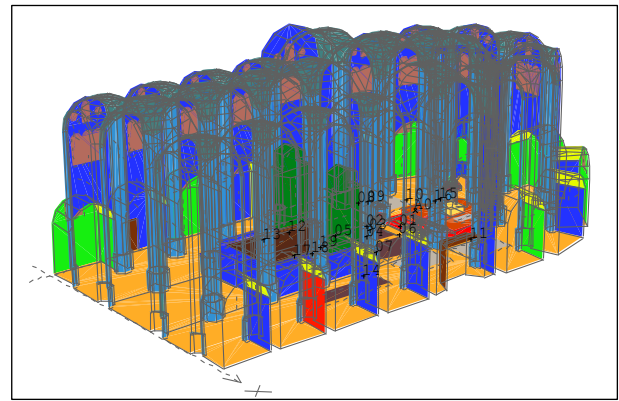


Figure 4. Geometrical 3D model created to simulate the acoustics of the cathedral.

makes use of the Randomized Tail-corrected Cone-tracing (RTC) algorithm with statistical corrections of the tail. This prediction method enables the calculation of numeric values for room acoustic parameters and the production of an echogram which can be used in the auralization processes. To mitigate the inconveniences of the method, the direct sound, the first-order specular and diffuse reflections, and the specular reflections of second order are handled in a deterministic way by the image source method. For the simulation carried out by CATT, the number of rays were determined automatically (85,148 rays) and a ray truncation time of 8 seconds was set.

Other acoustic calculations were carried out by using the TUCT (The Universal Cone Tracer) [13] motor where the acoustic parameters were obtained through processing echograms (E) and by processing the impulse response (h) algorithms. Specifically, the algorithm for closed-room "short calculation, basic auralization" with a "max split order" 1 was used, which determined the number of rays per cone automatically (206,061) for parameter calculation, and set the length of the impulse response at 8 seconds.

Figure 4 depicts the geometrical 3D model implemented for the cathedral with 3,463 planes, an approximate total volume of 118,500 m<sup>3</sup> and a surface of 27,190 m<sup>2</sup>. Table I shows the absorption coefficients from 125 to 4000 Hz octave bands associated to materials whose relative surface is greater than 0.8%, in addition to their colours assigned in the geometric three-dimensional model of Figure 4 and their references.

Likewise, flat or scarcely decorated surfaces are assigned scattering coefficients varying from 0.12 at 125 Hz to 0.17 at 4000 Hz, which include a linear increase of 0.01 to account for frequency

dependence. Shallow decorated surfaces are assigned higher scattering coefficients varying linearly from 0.20 at 125 Hz to 0.40 at 4000 Hz. Finally, pews, sculptures, and coffered vaults are assigned scattering coefficients varying from 0.30 at 125 Hz up to 0.80 at 4000 Hz [7].

The simulations undertaken use a calibration process based on an adjustment of the values of absorption coefficients of columns and stone walls of the cathedral such that the spatially averaged simulated reverberation times differ, on average, by no more than 5% from those measured on site, which are spatially averaged in the main congregational zones (pew and chair zones) (Table II). The limit for these differences is based on the just noticeable difference (JND), for which a value of 5% is widely accepted [10]. Since CATT-Acoustic offers the possibility of evaluating the values of these reverberation times in an interactive way based on classic formulae, the adjustment procedure does not necessarily require a complete simulation in the first stages.

## 5. Results and discussion

Figure 5(a) and (b) shows a comparison of the spectral behaviour in octave bands of spatially averaged values in the congregational areas, (reception points where direct sound failed to reach and those inside the reverberation radius are omitted) of EDT, and  $D_{50}$  parameters, respectively. Their error bars are also plotted which take into account the spatial dispersion of the various receivers through standard deviation. For the sake of clarity, the error bars of the simulation by TUCT, which are of the same order as those of

Table II. Spatially averaged measured reverberation time ( $T_{av}$ ) used in the calibration of the model and adjusted values ( $T_{adj}$ ).













Freq. (Hz)	125	250	500	1000	2000	4000
$T_{av}$ (s)	7.93	7.41	7.32	6.54	4.94	3.48
$T_{adj}$ (s)	7.99	7.56	7.41	6.72	5.08	3.32

CATT results, are omitted. It is worth highlighting the good agreement between the predicted results from any of the three algorithms of calculation of the acoustic parameters, and the acceptable concordance between experimental values on site and the simulations, particularly the results of the EDT parameter which are notoriously difficult to predict and where the dispersion is mainly at low frequencies. A further quantitative analysis of the discrepancies between the actual and virtual values of the acoustic parameters is outlined below.

Regarding the behaviour of the acoustic parameters in the 1 kHz band as a function of source-receiver distance, Figure 6(a) and (b) depicts the comparison between measured and simulated results (CATT results), for  $T_s$  and  $C_{80}$ , respectively. As a standard reference, the curves predicted by Barron's hypothesis of sound propagation [15] are superimposed. The plotted graphs indicate an acceptable agreement between experimental and simulated values at the various reception points and that the two set of results follow the trend marked by Barron's theoretical predictions within the range of source-receiver distances shown. At greater distances, higher deviations are expected.

To complete the analysis, Figure 7 shows the absolute differences between measured and simulated values for the reception points in the

Table I. Absorption coefficients and colour code of the materials for the simulations at the various frequencies.

Material	Fractional Area (%)	Colour code	Absorption coefficients					
			125 Hz	250 Hz	500 Hz	1 kHz	2 kHz	4 kHz
Columns*	24.6		0.16	0.18	0.16	0.16	0.17	0.17
Stone walls*	24.2		0.04	0.04	0.03	0.04	0.05	0.05
Domes and arches, [7]	18.0		0.04	0.04	0.05	0.05	0.06	0.06
Marble floor, [2]	11.2		0.01	0.01	0.02	0.02	0.03	0.03
Altarpieces in chapels, [7]	5.2		0.12	0.12	0.15	0.15	0.18	0.18
Chapels, [7]	4.6		0.04	0.04	0.05	0.05	0.06	0.06
Stained-glass windows, [14]	4.0		0.35	0.25	0.18	0.12	0.07	0.04
Organ (estimated)	2.0		0.12	0.14	0.16	0.16	0.16	0.16
Wooden pews, [2]	1.3		0.10	0.15	0.18	0.20	0.20	0.20
Choir seating, [7]	1.1		0.12	0.12	0.15	0.15	0.18	0.18
Doors, [2]	1.0		0.14	0.10	0.06	0.08	0.10	0.10
Plastic chairs, [2]	0.8		0.06	0.10	0.10	0.20	0.30	0.20

(\*) Adapted from the experimental results.

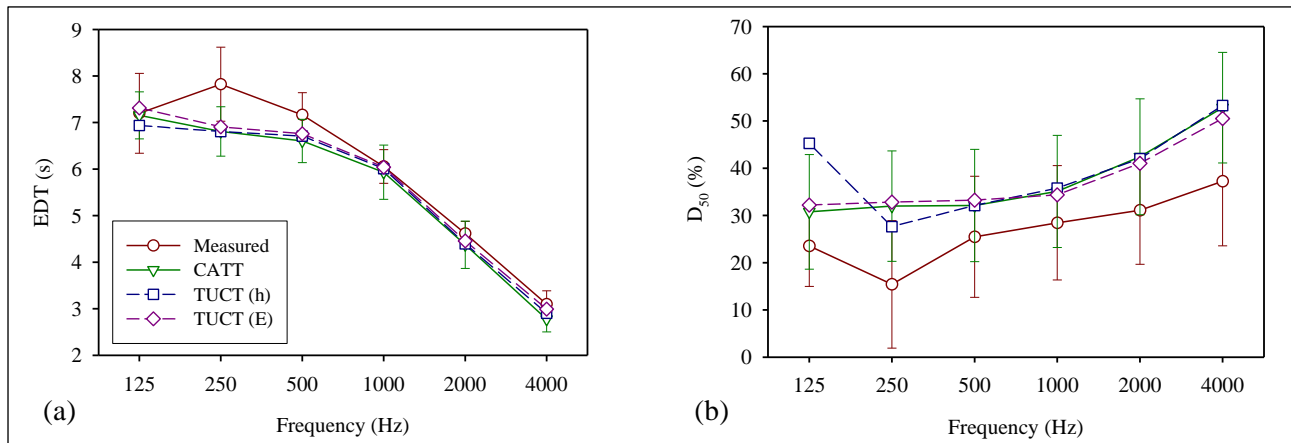


Figure 5. Spatially averaged results of EDT (a), and  $D_{50}$  (b) parameters, both measured and simulated with the different algorithms for each octave band. The vertical bars indicate the spatial dispersion of the parameters by means of SD.

cathedral and for each acoustic parameter in the six frequency octave bands. Accuracy between the two sets of values is within the range of 1-2 times the JNDs [8]. According to Martellotta [16], for enclosures with longer reverberation times, the JND for  $T_S$  should be 8.5% of the reference value, and for  $C_{80}$ , 1.5 dB. The greatest failures occur at low and high frequencies for all the acoustic parameters. Nevertheless, it can be seen that the range of accuracy includes the majority of the reception points, thereby supporting the validity and reliability of the simulation and the methodology.

## 6. Conclusions

Three separate prediction models are used for the computer simulation. The results from the model shown are presented here, which, due to its geometrical simplicity, enables values to be

reached that are more consistent with the experimental results in the calibration process.

The three geometric prediction algorithms used in this study (CATT, TUCT (h) and TUCT (E)) lead to very similar results to those of the model implemented and to an acceptable correspondence with the values measured on site, both in terms of the spectral behaviour and in its dependence on source-receiver distance. From the study of the absolute differences of the acoustic parameters analysed at each microphone position and for each frequency, it can be inferred that, within the range of accuracy of the simulation which includes 1-2 times the JNDs, the majority of the receiving points are included.

Despite the good agreement between experimental and simulated results, more exhaustive on-site measurements are needed which involve additional acoustic descriptors, such as those related to spatial impression, and further positions of the

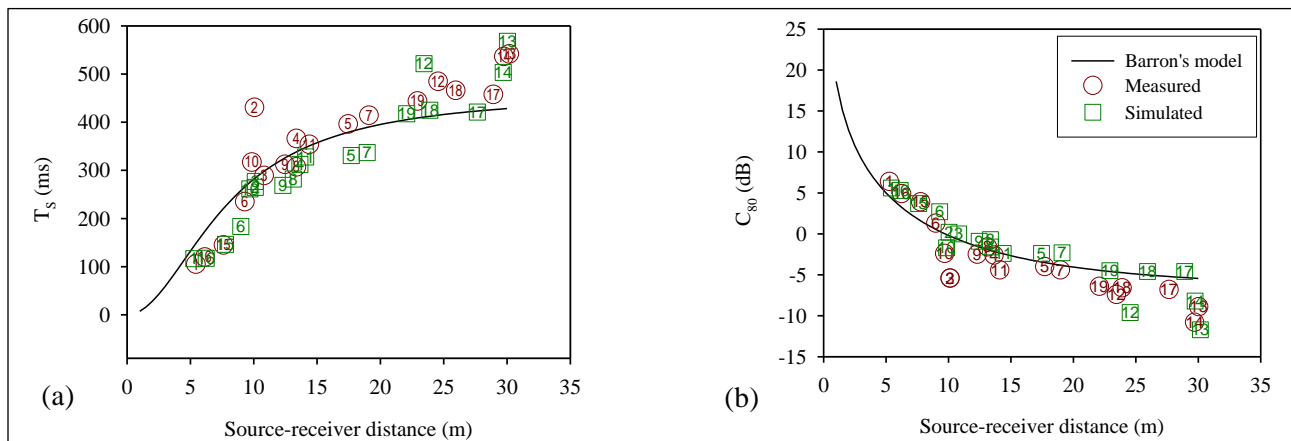


Figure 6. Results of  $T_S$  (a), and  $C_{80}$  (b) parameters, in the 1 kHz band, both measured and simulated with CATT versus source-receiver distance. The theoretical expected values according to Barron's model and the reception points are also shown.

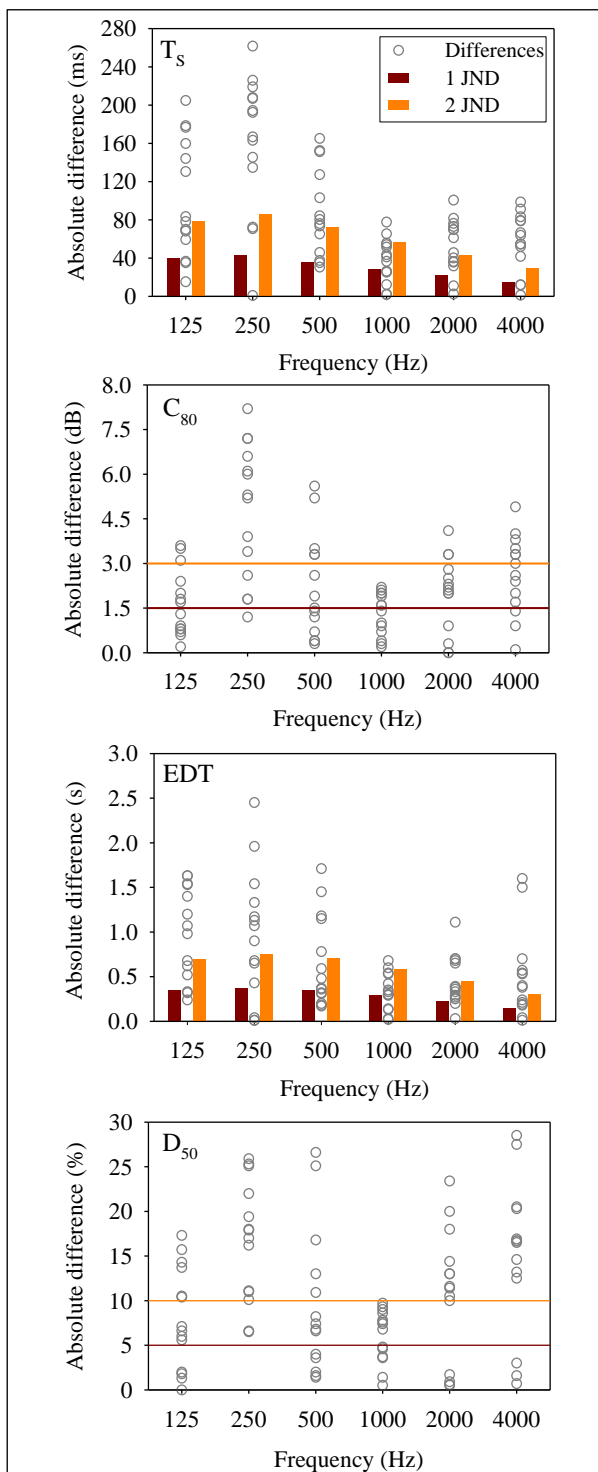


Figure 7. Absolute differences between measured and CATT-simulated results for the reception points, in the various octave bands, for each acoustic parameter. Two limits as a function of JND are indicated.

source and receiver are required in order to cover the entire ecclesial space. A new measurement campaign is currently being conducted which includes such aspects.

## Acknowledgements

The authors wish to express their appreciation for the valuable loan of the EASERA equipment from the department of Communication Engineering of the University of Malaga, and also to thank the Dean of the cathedral for allowing measurements to be carried out. This work has been financially supported by FEDER funds and the Spanish Ministry of Science and Innovation, with reference BIA2010-20523.

## References

- [1] J. H. Rindel: The use of computer modelling in room acoustics. *J. Vib. Eng.* 3 (2000) 219-224.
- [2] M. Vorländer: *Auralization, fundamentals of acoustics, modelling, simulation, algorithms and acoustic virtual reality.* Springer-Verlag, Berlin, 2008.
- [3] A. Krockstadt, S. Ström, S. Sörnsdal: Calculating the acoustical room response by the use of a ray-tracing technique. *J. Sound Vib.* 8 (1968) 118-125.
- [4] I. A. Drumm, Y. W. Lam: The adaptive beam-tracing algorithm. *J. Acoust. Soc. Am.* 107 (2000) 1405-1412.
- [5] T. A. Lewers: Combined beam tracing and radiant exchange computer model of room acoustics. *Appl. Acoust.* 38 (1993) 161-178.
- [6] M. Vorländer: Simulation of the transient and steady-state sound propagation in rooms using a new combined ray-tracing/image-source algorithm. *J. Acoust. Soc. Am.* 86 (1989) 172-178.
- [7] F. Martellotta: Identifying acoustical coupling by measurements and prediction-models for St. Peter's Basilica in Rome. *J. Acoust. Soc. Am.* 126 (2009) 1175-1186.
- [8] M. Galindo, T. Zamarreño, S. Girón: Acoustic simulations of Mudejar-Gothic churches. *J. Acoust. Soc. Am.* 126 (2009) 1207-1218.
- [9] T. Sauret: *La catedral de Málaga* (in Spanish). Servicio de publicaciones de la diputación, Málaga, 2003.
- [10] International Organization for Standardization ISO 3382-1:2009(E): *Acoustics-Measurement of room acoustic parameters. Performance rooms.* Geneva, Switzerland, 2009.
- [11] EASERA Tutorial v1.1. Software Design Ahnert GmbH, Berlin, 2006.
- [12] B-I. Dalenbäck: *CATT-Acoustic v8 user's manual.* CAT Technique, Gothenburg, Sweden, 2007.
- [13] B-I. Dalenbäck: *CATT TUCT v1.0 user's manual.* CAT Technique, Gothenburg, Sweden, 2010.
- [14] T. J. Cox, P. D'Antonio: *Acoustic absorber and diffusers, theory, design and application.* Spon, London, 2004.
- [15] T. Zamarreño, S. Girón, M. Galindo: Acoustic energy relations in Mudejar-Gothic churches. *J. Acoust. Soc. Am.* 121 (2007) 234-250.
- [16] F. Martellotta: The just noticeable difference of center time and clarity index in large reverberant spaces. *J. Acoust. Soc. Am.* 128 (2010) 654-663.